

THE IMPACT OF MASS SEGREGATION AND STAR-FORMATION ON THE RATES
OF GRAVITATIONAL-WAVE SOURCES FROM EXTREME MASS RATIO INSPIRALS

DANOR AHARON & HAGAI B. PERETS

Physics Department, Technion - Israel Institute of Technology, Haifa, Israel 3200003

Draft version March 5, 2018

Abstract

Compact stellar objects inspiralling into massive black holes (MBHs) in galactic nuclei are some of the most promising gravitational wave (GWs) sources for next generation GW-detectors. The rates of such extreme mass ratio inspirals (EMRIs) depend on the dynamics and distribution of compact objects around the MBH. Here we study the impact of mass-segregation processes on EMRI rates. In particular, we provide the expected mass function of EMRIs, given an initial mass function of stellar BHs (SBHs), and relate it to the mass-dependent detection rate of EMRIs. We then consider the role of star formation on the distribution of compact objects and its implication on EMRI rates. We find that the existence of a wide spectrum of SBH masses lead to the overall increase of EMRI rates, and to high rates of the EMRIs from the most-massive SBHs. However, it also leads to a relative quenching of EMRI rates from lower-mass SBHs, and together produces a steep dependence of the EMRI mass function on the highest-mass SBHs. Star-formation history plays a relatively small role in determining the EMRI rates of SBHs, since most of them migrate close to the MBH through mass-segregation rather than forming in-situ. However, the EMRI rate of neutron stars can be significantly increased when they form in-situ close to the MBH, as they can inspiral before relaxation processes significantly segregates them outwards. A reverse but weaker effect of decreasing the EMRI rates from neutron stars and white dwarfs occurs when star-formation proceeds far from the MBH.

1. INTRODUCTION

Nuclear stellar clusters, (NSCs) hosting massive black holes (MBHs) are thought to exist in a significant fraction of all galactic nuclei, including our own (Eisenhauer et al. 2005; Ghez et al. 2005). The dynamics of stars in the dense NSC lead to strong interactions between stars and the MBH. In particular compact objects (COs) such as white dwarfs (WDs), neutron stars (NSs), and stellar black holes (SBHs), may inspiral onto the MBH and emit gravitational waves (GWs) observable to cosmological distances with next generation GW detectors. The inspiral of a CO into an MBH (“extreme mass ratio inspiral” [EMRI]) is among the main targets of future Evolved Laser Interferometer Space Antenna (eLISA).

The properties of EMRIs and their rates depend strongly on the evolution and dynamics of different stellar populations near MBHs, processes in which mass segregation processes play a key role (see Freitag et al. keshet 2006; Hopman and Alexander keshet 2006b; Alexander and Hopman keshet 2009; Keshet et al. keshet 2009; Preto and Amaro-Seoane keshet 2010 and Amaro-Seoane and Preto (2011) for a detailed treatment of mass segregation near MBHs). Mass segregation occurs through two-body interactions between less massive and more massive objects. The encounters drive stellar populations of different masses towards energy equipartition which results in the more massive objects migrating closer to the center, while the less massive ones migrate outwards. In particular, mass segregation can increase the density of the more massive COs within the region $r < a_{GW}$, where a_{GW} is the maximal semi-major axis at which a CO could still inspiral and become an eLISA source (hereafter the critical separation), rather than plunge-in on a too radial orbit and spending too short time in the GW detector band and

unlikely to be detected. Hopman and Alexander (2005) derived an analytical order-of-magnitude estimate for the critical separation, given by

$$a_{GW} = r_h \left(\frac{d_c}{r_h} \right)^{3/(3-2p)} \quad (1)$$

where r_h is the radius of influence (see section 3), d_c is a length scale and p is the power law of the distribution function ($f(E, t) \sim E^p$, see section 3 and Bahcall and Wolf 1976).

The event rate of EMRIs has been estimated by several studies (e.g. Hils and Bender (1995); Sigurdsson and Rees (1997); Freitag (2001); Ivanov (2002); Alexander and Hopman (2003); Hopman and Alexander (2006b)) but remains rather uncertain, in part because of the slow nature of the inspiral process, which occurs on many dynamical times (see further discussion by Hopman and Alexander (2006b)).

Previous studies of EMRI rates in NSCs typically considered only populations of single-mass SBHs (with mass $m_\bullet = 10 M_\odot$), however, theoretical studies, and the recent GW detection of a merger of two $\sim 30 M_\odot$, suggest a potentially wide range of SBH masses. The effect of such non-trivial SBH population on the rates of GWs from merger of binary-SBH (detectable by aLIGO) was considered by O’Leary et al. (2009). Here we focus on the implications for a different type of GW sources, namely inspirals of COs on MBHs, producing EMRIs. Future EMRI detections could potentially probe the mass function (MF) of inspiralling SBHs. However, the mutual interactions between SBHs and stars of different masses could significantly alter their distributions near MBHs, and thereby the EMRI rate from SBHs

of different masses. Therefore, translating the EMRI MF into the original MF of SBHs requires understanding the non-trivial evolution and mass segregation processes in NSCs. Finally, we note that not only the MF of SBHs change their distribution, but potentially the star-formation history and build-up of the NSC (see Perets and Mastrobuono-Battisti 2014; Antonini 2014; Aharon and Perets 2015; Aharon et al. 2016).

In this letter, we explore for the first time the expected mass-function of EMRIs (with the main focus on SBHs), and its relation and translation to the general MF of SBHs. Furthermore, we consider both the rates from relaxed NSCs, as well the role of the build-up and star-formation history in affecting the EMRI properties and rates.

2. ANALYTIC DERIVATION OF EMRI RATES IN RELAXED NUCLEAR CLUSTERS

In relaxed NSC systems the distribution of different stellar populations can typically achieve a steady state. Studies of simple stellar populations (composed of 4 populations: Solar mass main sequence (MS) stars, $1.4 M_{\odot}$ NSs, $0.6 M_{\odot}$ WDs and $10 M_{\odot}$ SBHs), using Fokker-Planck (FP; see also below), Monte-Carlo or N-body simulations showed them to be distributed with power-law density profiles, generally consistent with analytic estimates of mass-segregation effects near MBH by Bahcall and Wolf (1977). Later studies (Alexander and Hopman 2009) pointed-out that the mass-segregation solution for the steady-state distribution of stars around a MBH has two branches: a weak-segregation solution (described by Bahcall and Wolf 1977) and a different, strong-segregation solution. They found that their properties depends on the heavy-to-light stellar mass ratio M_H/M_L and on the unbound population number ratio N_H/N_L , through the relaxational coupling parameter

$$\Delta = 4N_H M_H^2 / [N_L M_L^2 (3 + M_H/M_L)], \quad (2)$$

where systems with $\Delta \lesssim 1$ reside in the strong mass-segregation regime. In the strong mass-segregation regime the massive objects can achieve much steeper density profile compared with the Bahcall and Wolf (1977) weak mass-segregation regime. Alexander and Hopman (2009) mainly focused on cases which can be generally divided between small population of massive objects ($M_H \sim 10 M_{\odot}$ SBHs) and large population of low-mass objects (MS stars, NSs and WDs with $M_L \sim 1 M_{\odot}$) in the $\Delta < 1$ regime. However, a more complex situation arises when the high-mass population is composed of a range of masses. For example, in the case of two massive populations (with M_{H1} , M_{H2} and N_{H1} , N_{H2}), the calculated Δ parameter could be below unity when comparing each of the high-mass populations to the low-mass one, while Δ could be above unity when comparing the two massive-stars populations (i.e. treating M_{H2} as a low mass compared with M_{H1}). Keshet et al. (2009) used analytic tools and generalized the derivation for such non-trivial MF cases.

Using the above mentioned results, one can find the expected density profile ($n(r) \propto r^{-\gamma}$), where $\gamma = p + 3/2$, then for a given population of stars with a given mass in a relaxed NSC, given by (Keshet et al. 2009) and Alexander and Hopman (2009):

$$p(m) \simeq m/4M_0 \quad (3)$$

where m is the relevant population mass and M_0 is the weight average mass. For mass function not strongly dominated by light stars (negligible flow) the relation is linear: $p \propto m$ (Bahcall and Wolf 1977; Keshet et al. 2009). In order to find the number of GW progenitors we then need to integrate the number of CO GW progenitors (i.e. inside the critical separation, a_{GW}):

$$\Gamma \sim \int^{a_{GW}} r^{-\gamma} d^3r \sim a_{GW}^{3/2-p}. \quad (4)$$

Substituting Eq. 1 then gives us the inspiral rate dependence on the the CO mass per unit mass:

$$\Gamma(m)dm \sim a_{GW}^{\frac{3}{2}-\frac{m}{4M_0}} = \left(r_h \left(\frac{d_c}{r_h} \right)^{3/(3-\frac{m}{2M_0})} \right)^{\frac{3}{2}-\frac{m}{4M_0}} dm \quad (5)$$

Given the GW detector sensitivity on the inspiraling CO mass, COs with $M_1 > M_2$ would be detected to distances larger by M_2/M_1 and taking a homogenous universe at sufficiently large distances one expects a $(M_2/M_1)^3$ enhancement in the detection rate. Given an intrinsic MF of COs (for simplicity assuming a power-law distribution; $\xi(m) \propto m^{-\beta}$), we can now combine all of the above EQs together and relate the CO intrinsic MF to the MF of detected EMRIs:

$$N(m) \sim \int \left(r_h \left(\frac{d_c}{r_h} \right)^{3/(3-\frac{m}{2M_0})} \right)^{\frac{3}{2}-\frac{m}{4M_0}} m^{-\beta} dm \quad (6)$$

where the last integral can be numerically solved. Given sufficient number of EMRI detection one can use these relation to derive the intrinsic MF of SBH.

3. NUMERICAL CALCULATIONS USING A FOKKER-PPLANCK APPROACH

In order to test the analytic results we use a FP approach. Our model is based on the classic approach of Bahcall and Wolf (1976) and Bahcall and Wolf (1977) to the problem, and use our parallelized FP code (as described in Aharon and Perets 2015; Aharon et al. 2016). We simulate the evolution in time, t , of the energy, E , distribution function (DF) - $f(E, t)$ and the number density of stars in a spherical system around a MBH. The DF represents the distribution of stars in central few pcs, and in particular in the range between the Schwarzschild radius and the radius of influence. To our original code we now added the treatment of multi-mass cases, following the same equations as described in Bahcall and Wolf (1977) and Hopman and Alexander (2006b).

In the following, we briefly recapitulate the main assumptions and discuss our treatment of GW capture.

3.1. Fokker-Planck analysis

The FP model used consists of a time and energy-dependent, angular momentum-averaged particle conservation equation. It has the form:

$$\frac{\partial f(E, t)}{\partial t} = -AE^{-\frac{5}{2}} \frac{\partial F}{\partial E} - F_{LC}(E, T) + F_{SF}(E, T) \quad (7)$$

where

$$A = \frac{32\pi^2}{3} G^2 M_*^2 \ln(\Lambda) \quad (8)$$

The term $F = F[f(E), E]$ is related to the stellar flow, and plays an important role in the evolution of the stellar cluster. It presents the flow of stars in energy space due to two-body relaxation, it is defined by:

$$F = \int dE' \left(f(E) \frac{\partial f(E')}{\partial E'} - f(E') \frac{\partial f(E)}{\partial E} \right) (\max(E, E'))^{-\frac{3}{2}}. \quad (9)$$

We note that similar to Hopman and Alexander (2006b) work, we neglect here the effect of resonant relaxation (RR; Rauch and Tremaine 1996; Rauch and Ingalls 1998), which was suggested to increase the EMRI rate by up to an order of magnitude (Hopman and Alexander 2006a and Merritt (2015)). However, more recent analysis of (Bar-Or and Alexander 2016, who also considered Merritt work, Bar-Or, private communication), suggest a relatively negligible effect, supporting our approach on this issue.

3.2. NSC models

We followed the evolution of several types of NSCs with a MBH mass of $4 \times 10^6 M_\odot$ which can be a representative of a typical eLISA sources. We first studied primordial NSCs which achieved a steady state, and did not experience any star formation (SF). Such models correspond to the same type of models considered previously (e.g. Freitag et al. 2006; Hopman and Alexander 2006b), besides the difference in stellar population used (see next section; we also recalculated the same models used by Hopman and Alexander 2006b, and verified we get the same results in this case).

For the model with SF we tested two cases: inner SF formation in the range $0.05 - 0.5 \text{ pc}$ and outer SF between $2 - 3.5 \text{ pc}$. For each of these two cases we considered two different scenarios of formation and evolution: 1) in situ formation of MS stars and COs. 2) An initial pre-existing cusp of MS+CO stars evolved with continuous SF MS+CO stars (see Table 1). In the latter scenario, we define the initial MS DF within r_h in the form of $f(E_{r < r_h}, t_0) \propto E^{0.25}$ corresponding to the BW steady-state cusp which has the form of $n \propto r^{-7/4}$. The density profile at r_h is normalized to $4 \times 10^4 \text{ pc}^{-3}$, corresponding to number density at r_h in the galactic center (GC) assuming a mean mass of $1 M_\odot$ (Genzel et al. 2003). We also adopt the following parameters taken from the GC values: $\sigma_* = 75 \text{ km/s}$ and $r_h = 2 \text{ pc}$ (Genzel et al. 2003). We consider the DF at $r > r_h$ to have a Maxwellian distribution: $f(E_{r > r_h}, t) \propto e^{E/\sigma_*}$ (Bahcall and Wolf 1976).

In order to account for SF, following our previous work in Aharon and Perets (2015), we added the source term that represents the stars and CO formation in the form:

$$F_{SF}(E, T) = \frac{\partial}{\partial t} (\Pi(E) E_0 E^\alpha), \quad (10)$$

where $\Pi(E)$ is a rectangular function, which boundaries correspond to the region where new stars are assumed to form; E_0 is the source term amplitude; and F_{SF} is a power-law function with a slope α , defining the SF distribution in phase space.

3.3. Types of Stellar Objects

Similar to Hopman and Alexander 2006b we consider four basic populations. The first consists of MS stars, assumed here to be of solar mass. MSs do not contribute to the GW inspiral rate since they are tidally disrupted before spiraling in, but they do contribute dynamically. The other populations represent WDs ($M_{WD} = 0.6 M_\odot$), NSs ($M_{NS} = 1.4 M_\odot$), and SBHs. We considered cases which include stellar populations of $10 M_\odot$ SBHs (similar to previous studies), but also considered cases with both $10 M_\odot$ and $30 M_\odot$ SBHs, in order to probe the effect of more than a single type of massive objects. Considering Kroupa (2001) work, we used the fraction ratios of the four populations as $C_{MS} : C_{WD} : C_{NS} : C_{BH_{10M_\odot}} : C_{BH_{30M_\odot}} = 0.72 : 0.26 : 0.014 : 2.3 \times 10^{-3} : 2.2 \times 10^{-4}$, typical for continuously star-forming populations. The MF of SBHs is not well understood, however for SBHs up to $\sim 40 M_\odot$ theoretical models of direct collapse suggest an almost linear relation between progenitor mass and final SBH mass (Belczynski et al. 2016), and we therefore assume an SBH MF which goes like $\propto m^{-2.1}$ close to the initial MF of massive stars ($m^{-2.3}$).

4. RESULTS

4.1. Distribution of compact objects populations in NSCs

We followed the evolution of the studied NSCs for 10 Gyr corresponding to Hubble timescale. Note that this timescale is also comparable with the relaxation time for a GC-like NSC, but likely lower than the relaxation time for NSCs hosting more massive MBH. We present the density profile of the studied scenarios in Figs 1, and 2, where we focus the central 0.01 pc region to predict the GW rates (10^{-3} for WDs and NSs). We integrate the density profile in the mentioned region and obtain the number and derive the rates of inspiralling CO. We summarize our results in Table 1. For comparison we obtained results from simulations similar to those of Hopman and Alexander (2006; Fig. 1; i.e. a steady state NSC with no SF).

As expected from the effects of strong mass-segregation the density profile of the SBHs in most scenario is much steeper than the \sim Solar mass MS/CO stars. Consequently, the rates of EMRI of SBHs is the highest compared with NSs and WDs. In the inner regions of the NSC, SBHs can become the most frequent stellar species, where the exact region where the dominate depends on the specific model explored.

The distribution of the $10 M_\odot$ SBHs in NSCs that include $30 M_\odot$ SBHs is very similar to the NS distribution, where in NSCs without $30 M_\odot$ SBHs, the distribution of $10 M_\odot$ has the steeper slope compared to the other populations. In other words, in the absence of $30 M_\odot$ SBHs, the $10 M_\odot$ SBHs distribution is border-line between the weak and strong mass-segregation regimes. The existence of the $30 M_\odot$ population quenches the effects of strong mass-segregation on the $10 M_\odot$, and only the $30 M_\odot$ SBHs are strongly segregated.

The obtained slope of the $10 M_\odot$ SBH number density in the outer-SF scenario is $\gamma_{10M_\odot SBH}^{out} \approx 1.9$, where in the scenario that includes the $30 M_\odot$ SBHs it decreases to 1.42, and the slope of the more massive

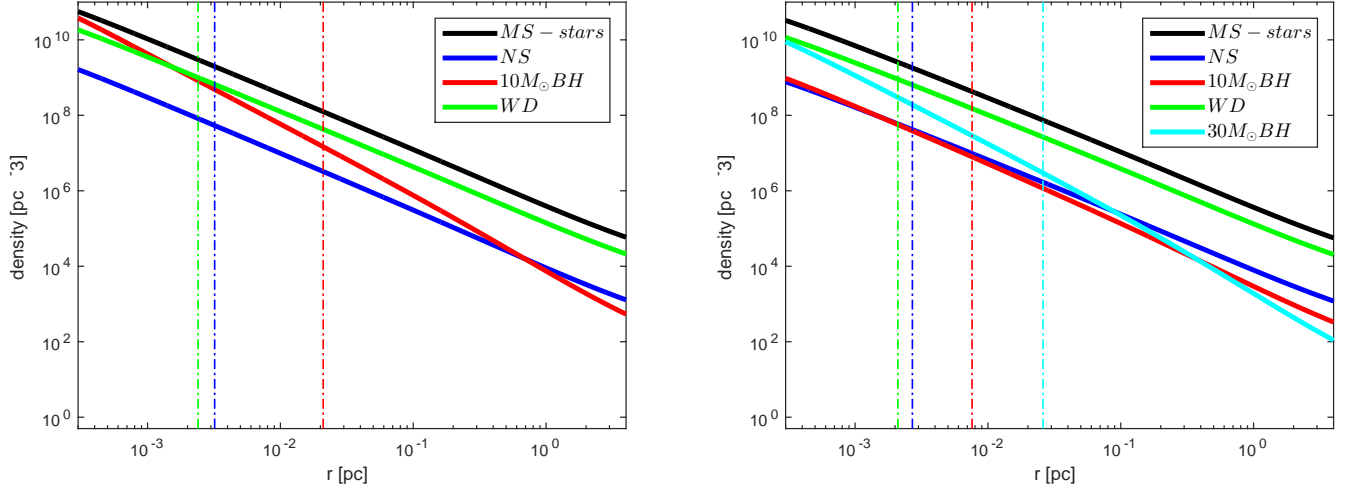


FIG. 1.— Density profile of a 10 Gyr evolved compact stellar objects. Left panel: pre-existing BW cusp with COs evolved from outer CO formation at distances $2 - 3.5$ pc from the MBH at the rates of 10^{-4} yr^{-1} for 4 different stellar populations (MSs, NSs, WDs and $10 M_{\odot}$ SBHs). The dashed dot vertical lines mark the maximal semimajor axis for each CO population where it experiences “successful inspiral”. For each population, the colors of the dashed dot lines are corresponding with the colors of its density profile. The relaxational coupling parameter for the $10 M_{\odot}$ is $\Delta \approx 0.87$. The power-laws for each population within its a_{GW} are $\gamma_{NS} = 1.4$, $\gamma_{WD} = 1.3$ and $\gamma_{10 M_{\odot} SBH} = 1.9$. Right panel: similar NSC, with the addition of stellar population composed of $30 M_{\odot}$ SBHs. The relaxational coupling parameter for the $30 M_{\odot}$ is $\Delta \approx 0.08$, and the power-laws are $\gamma_{NS} = 1.3$, $\gamma_{WD} = 1.3$, $\gamma_{10 M_{\odot} SBH} = 1.4$ and $\gamma_{30 M_{\odot} SBH} = 2.1$.

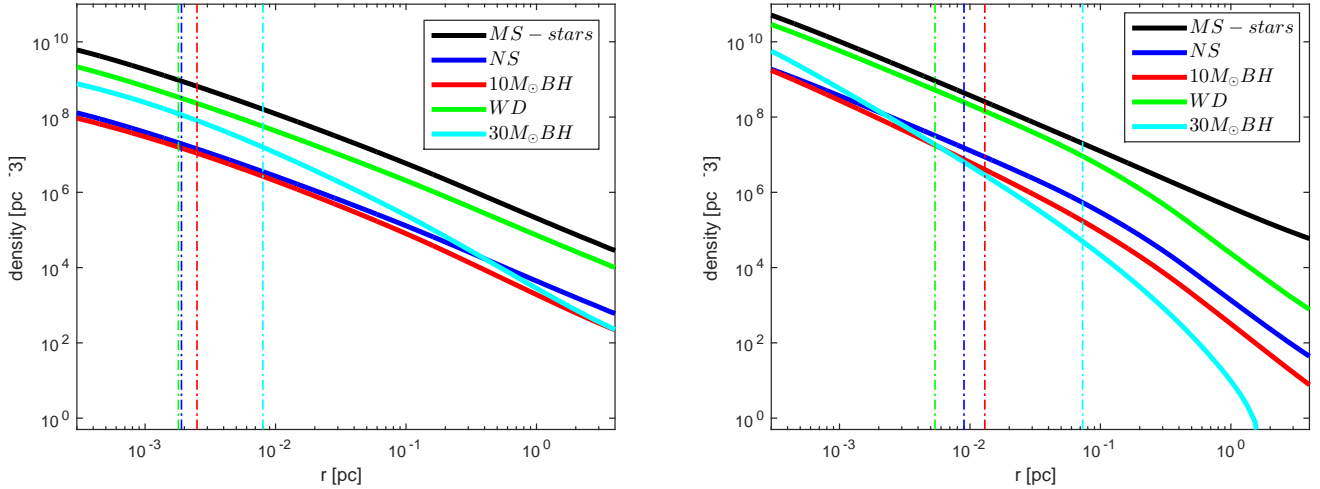


FIG. 2.— Two other GW predicted scenarios. Left panel: Density profile of NSCs evolved through in situ SF with a rate of $5 \times 10^{-4} \text{ yr}^{-1}$ (built up NSC) in the outer region ($2 - 3.5$ pc). The relaxational coupling parameter for the $30 M_{\odot}$ is $\Delta \approx 5.92$. The power-laws are $\gamma_{NS} = 1.0$, $\gamma_{WD} = 1.0$, $\gamma_{10 M_{\odot} SBH} = 1.0$ and $\gamma_{30 M_{\odot} SBH} = 1.1$. Right panel: CO formation in the inner region ($0.05 - 0.5$ pc) in NSC that evolves from pre-existing cusp. The relaxational coupling parameter for the $30 M_{\odot}$ is $\Delta \approx 0.03$, and the power-laws for each population within its a_{GW} are $\gamma_{NS} = 1.3$, $\gamma_{WD} = 1.3$, $\gamma_{10 M_{\odot} SBH} = 1.5$ and $\gamma_{30 M_{\odot} SBH} = 2.3$.

SBHs is $\gamma_{30 M_{\odot} SBH}^{out} \approx 1.9$ (Fig. 1). The highest slope ($\gamma_{30 M_{\odot} SBH}^{out} \approx 2.3$) is obtained for the $30 M_{\odot}$ SBH population in NSCs, evolved from pre-existing stellar cusp, that experience inner-SF. The slopes calculated in our numerical simulations are consistent with the analytical study of Keshet et al. (2009). We emphasize that we also tested EMRI rates model with a range of SBH masses in order to verify our Analytic derivation of the rates presented in section 2, and found comparable results.

4.2. EMRI rates

Following the obtained NSC stellar distribution, we integrated the number of COs up to the critical separa-

tion in order to quantify the number of expected EMRIs. We summarize the results in Table 1. The highest EMRIs are obtained in NSCs that evolve from a pre-existing cusp that also experiences strong SF in the outer region. The lowest overall rates are obtained with inner-SF that builds up the NSC. For comparison with previous studies, the last row in the table is based on Hopman and Alexander (2006b) as described in 4.1.

5. SUMMARY

In this work we studied the rates of GWs from extreme-mass ratio inspirals, but considered two novel aspects which were little, or not considered before in this context. We study (1) the impact of a wide mass-spectrum

scenario	CO formation rate (yr^{-1})	Γ_{NS} (Gyr^{-1})	Γ_{WD} (Gyr^{-1})	$\Gamma_{SBH_{10M_{\odot}}}$ (Gyr^{-1})	$\Gamma_{SBH_{30M_{\odot}}}$ (Gyr^{-1})
pre-existing cusp outer formation without $30M_{\odot}$ SBH	10^{-4}	14	79	232	-
pre-existing cusp outer formation		11	71	92	265
pre-existing cusp inner formation		15	73	87	252
outer in-situ formation		7	22	58	273
inner in-situ formation		39	62	74	312
outer in-situ formation	5×10^{-4}	32	112	62	288
inner in-situ formation		45	68	85	301
pre-existing cusp inner formation		8	67	15	97
relaxed cusp	-	7	73	89	273
relaxed cusp without $30M_{\odot}$ SBH (based on Hopman and Alexander 2006b)	-	6	33	252	-

TABLE 1
NSC MODEL AND THE PREDICTED GW RATES

SBHs (as suggested by theoretical work and the recent detections of high mass SBHs by aLIGO; Abbott et al. 2016; Belczynski et al. 2016) on EMRI rates, and (2) the role of in-situ formation of stars and COs during the build-up and/or formation of nuclear stellar clusters.

Our main findings are as follows:

1. We find that strong mass-segregation produces a steep power-law density profile for the most massive SBHs, but at the same time quenches the migration of less massive SBHs close to the MBH. We quantify this effect and provide a translation between the intrinsic mass function of CO, in particular SBHs, and the (future) observable mass function of the EMRI GW sources, showing the latter to be strongly biased towards high mass COs.
2. We find that SF plays a relatively small role in eventually determining the EMRI rates for SBHs (and its mass function), since most of them migrate close to the MBH through mass-segregation rather

than form in-situ. However, the rate of EMRI of neutron stars can be significantly increased when they form in-situ close to the MBH. In this latter case neutron stars can inspiral before relaxation processes significantly segregates them outwards farther away from the MBH. A reverse but weaker effect of decreasing the EMRI rates from neutron stars and white dwarfs occurs when star-formation proceeds far from the MBH. In this case the mass segregation processes due to the SBHs somewhat quench the newly formed NSs/WDs from diffusing into the inner regions, and lower their EMRI rates.

We would like to thank Clovis Hopman the use of the basic components in his FP code for developing the FP code used in our simulations. We acknowledge support from the I-CORE Program of the Planning and Budgeting Committee and The Israel Science Foundation grant 1829/12, as well support from the Asher Space Research Institute in the Technion.

REFERENCES

- B. P. Abbott, R. Abbott, T. D. Abbott, M. R. Abernathy, F. Acernese, K. Ackley, C. Adams, T. Adams, P. Addesso, R. X. Adhikari, and et al. Observation of Gravitational Waves from a Binary Black Hole Merger. *Physical Review Letters*, 116(6): 061102, February 2016. doi:10.1103/PhysRevLett.116.061102.
- D. Aharon and H. B. Perets. Formation and Evolution of Nuclear Star Clusters with In Situ Star Formation: Nuclear Cores and Age Segregation. *ApJ*, 799:185, February 2015. doi:10.1088/0004-637X/799/2/185.
- D. Aharon, A. Mastrobuono Battisti, and H. B. Perets. The History of Tidal Disruption Events in Galactic Nuclei. *ApJ*, 823:137, June 2016. doi:10.3847/0004-637X/823/2/137.
- T. Alexander and C. Hopman. Orbital In-spiral into a Massive Black Hole in a Galactic Center. *ApJ*, 590:L29–L32, June 2003. doi:10.1086/376672.
- T. Alexander and C. Hopman. Strong Mass Segregation Around a Massive Black Hole. *ApJ*, 697:1861–1869, June 2009. doi:10.1088/0004-637X/697/2/1861.
- P. Amaro-Seoane and M. Preto. The impact of realistic models of mass segregation on the event rate of extreme-mass ratio inspirals and cusp re-growth. *Classical and Quantum Gravity*, 28(9):094017, May 2011. doi:10.1088/0264-9381/28/9/094017.
- F. Antonini. On the Distribution of Stellar Remnants around Massive Black Holes: Slow Mass Segregation, Star Cluster Inspirals, and Correlated Orbits. *ApJ*, 794:106, October 2014. doi:10.1088/0004-637X/794/2/106.
- J. N. Bahcall and R. A. Wolf. Star distribution around a massive black hole in a globular cluster. *ApJ*, 209:214–232, October 1976. doi:10.1086/154711.
- J. N. Bahcall and R. A. Wolf. The star distribution around a massive black hole in a globular cluster. II Unequal star masses. *ApJ*, 216:883–907, September 1977. doi:10.1086/155534.
- B. Bar-Or and T. Alexander. Steady-state Relativistic Stellar Dynamics Around a Massive Black hole. *ApJ*, 820:129, April 2016. doi:10.3847/0004-637X/820/2/129.
- K. Belczynski, A. Heger, W. Gladysz, A. J. Ruiter, S. Woosley, G. Wiktorowicz, H.-Y. Chen, T. Bulik, R. O’Shaughnesy, D. E. Holz, C. L. Fryer, and E. Berti. The Effect of Pair-Instability Mass Loss on Black Hole Mergers. *ArXiv e-prints*, July 2016.
- F. Eisenhauer, R. Genzel, T. Alexander, R. Abuter, T. Paumard, T. Ott, A. Gilbert, S. Gillessen, M. Horrobin, S. Trippe, H. Bonnet, C. Dumas, N. Hubin, A. Kaufer, M. Kissler-Patig, G. Monnet, S. Ströbele, T. Szeifert, A. Eckart, R. Schödel, and S. Zucker. SINFONI in the Galactic Center: Young Stars and Infrared Flares in the Central Light-Month. *ApJ*, 628:246–259, July 2005. doi:10.1086/430667.

- M. Freitag. Monte Carlo cluster simulations to determine the rate of compact star inspiralling to a central galactic black hole. *Classical and Quantum Gravity*, 18:4033–4038, October 2001. doi:10.1088/0264-9381/18/19/309.
- M. Freitag, P. Amaro-Seoane, and V. Kalogera. Stellar Remnants in Galactic Nuclei: Mass Segregation. *ApJ*, 649:91–117, September 2006. doi:10.1086/506193.
- R. Genzel, R. Schödel, T. Ott, F. Eisenhauer, R. Hofmann, M. Lehnert, A. Eckart, T. Alexander, A. Sternberg, R. Lenzen, Y. Clénet, F. Lacombe, D. Rouan, A. Renzini, and L. E. Tacconi-Garman. The Stellar Cusp around the Supermassive Black Hole in the Galactic Center. *ApJ*, 594:812–832, September 2003. doi:10.1086/377127.
- A. M. Ghez, S. Salim, S. D. Hornstein, A. Tanner, J. R. Lu, M. Morris, E. E. Becklin, and G. Duchêne. Stellar Orbits around the Galactic Center Black Hole. *ApJ*, 620:744–757, February 2005. doi:10.1086/427175.
- D. Hils and P. L. Bender. Gradual approach to coalescence for compact stars orbiting massive black holes. *ApJ*, 445:L7–L10, May 1995. doi:10.1086/187876.
- C. Hopman and T. Alexander. The Orbital Statistics of Stellar Inspirals and Relaxation near a Massive Black Hole: Characterizing Gravitational Wave Sources. *ApJ*, 629:362–372, August 2005. doi:10.1086/431475.
- C. Hopman and T. Alexander. Resonant Relaxation near a Massive Black Hole: The Stellar Distribution and Gravitational Wave Sources. *ApJ*, 645:1152–1163, July 2006a. doi:10.1086/504400.
- C. Hopman and T. Alexander. The Effect of Mass Segregation on Gravitational Wave Sources near Massive Black Holes. *ApJ*, 645:L133–L136, July 2006b. doi:10.1086/506273.
- P. B. Ivanov. On the formation rate of close binaries consisting of a super-massive black hole and a white dwarf. *MNRAS*, 336:373–381, October 2002. doi:10.1046/j.1365-8711.2002.05733.x.
- U. Keshet, C. Hopman, and T. Alexander. Analytic Study of Mass Segregation Around a Massive Black Hole. *ApJ*, 698:L64–L67, June 2009. doi:10.1088/0004-637X/698/1/L64.
- P. Kroupa. On the variation of the initial mass function. *MNRAS*, 322:231–246, April 2001. doi:10.1046/j.1365-8711.2001.04022.x.
- D. Merritt. Gravitational Encounters and the Evolution of Galactic Nuclei. IV. Captures Mediated by Gravitational-wave Energy Loss. *ApJ*, 814:57, November 2015. doi:10.1088/0004-637X/814/1/57.
- R. M. O’Leary, B. Kocsis, and A. Loeb. Gravitational waves from scattering of stellar-mass black holes in galactic nuclei. *MNRAS*, 395:2127–2146, June 2009. doi:10.1111/j.1365-2966.2009.14653.x.
- H. B. Perets and A. Mastrobuono-Battisti. Age and Mass Segregation of Multiple Stellar Populations in Galactic Nuclei and their Observational Signatures. *ApJ*, 784:L44, April 2014. doi:10.1088/2041-8205/784/2/L44.
- M. Preto and P. Amaro-Seoane. On Strong Mass Segregation Around a Massive Black Hole: Implications for Lower-Frequency Gravitational-Wave Astrophysics. *ApJ*, 708:L42–L46, January 2010. doi:10.1088/2041-8205/708/1/L42.
- K. P. Rauch and B. Ingalls. Resonant tidal disruption in galactic nuclei. *MNRAS*, 299:1231–1241, October 1998. doi:10.1046/j.1365-8711.1998.01889.x.
- K. P. Rauch and S. Tremaine. Resonant relaxation in stellar systems. *New Astronomy*, 1:149–170, October 1996. doi:10.1016/S1384-1076(96)00012-7.
- S. Sigurdsson and M. J. Rees. Capture of stellar mass compact objects by massive black holes in galactic cusps. *MNRAS*, 284:318–326, January 1997. doi:10.1093/mnras/284.2.318.